Application of Uncertainty Visualization Methods to Meteorological Trajectories

Ryan A. Boller, Scott A. Braun, Jadrian J. Miles, and David H. Laidlaw

Abstract— We present applications of uncertainty visualization methods to a global meteorological model, allowing better understanding of the composition of the local environment of developing hurricanes. Our work enables efficient visual pruning of unlikely results, especially in regions of atmospheric shear. We derive bounds on advection uncertainty due to interpolation and incorporate this uncertainty into our visualization of trajectories, facilitating visual pruning. By identifying trajectories that indicate a protection of storm's core from outside influence, we also attempt to corroborate the viability of a recently devised meteorological theory that hurricanes develop in protected, "marsupial" pouches.

Index Terms—Uncertainty visualization, multi-field visualization, flow visualization, time-varying data, meteorological visualization techniques.

--- ✦ ---

1 INTRODUCTION

This paper describes the application of uncertainty visualization methods to meteorological flow. The driving goal of this work is to improve hurricane prediction through a better understanding of the interaction of a storm and its local environment. Some important factors in this understanding are the air's source, path, and composition. These properties can be neatly encapsulated and represented by trajectories, otherwise known as pathlines or particle paths.

These trajectories begin, or are "seeded," as a set of particles at a user-specified location in space and time, then travel through a time-varying vector field. In meteorological studies, this initial volume of seeds is known as an air parcel; the vector field is the air-parcel 3-dimensional velocity. The concept of backward trajectories [1] is applied to this problem since we know the "final" position of air we are interested in: that which is near developing hurricanes. Therefore we seed the air parcel trajectories near the storm and work backward through time and space to determine the source and path the air took to its final position. Along the way, we can also maintain "snapshots" in time of the path's properties, such as its relative humidity.

While these analyses provide a good approximation of the air parcels' paths, the oft-overlooked problem of identifying and representing sources of potential uncertainty [2] is addressed. The pathlines are a derived quantity, but the accuracy of their derivations [3] is rarely represented. We provide an upper bound and visual representation for the uncertainty of these calculations. The aim is to prevent the user from reaching erroneous conclusions about the storm and its environment based upon trajectories with a high degree of uncertainty resulting from passage of air parcels through regions of sharp velocity gradients or errors associated with the underlying interpolation. It also facilitates the efficient visual pruning of unlikely results by allowing the user to disregard trajectories with higher uncertainty.

As mentioned above, these uncertainty estimates are especially important in regions of high wind shear that are common near the extreme conditions surrounding a hurricane. Since these adjacent vectors are rapidly changing direction and magnitude, the resulting trajectories that flow through them have a higher level of uncertainty than those that flow through a more uniform field. Therefore, without the user inspecting the underlying vector fields for each time step along the trajectories' paths, there is no way of understanding their corresponding level of confidence.

A final related factor is the resolution of the underlying data. In this work, we use global atmospheric analyses produced by the National Oceanic and Atmospheric Administration's National Centers for Environmental Prediction. The analyses contain information on atmospheric temperature, pressure, humidity, and 3-dimensional air velocities with a spatial resolution of 1° latitude and longitude available at six-hour increments. Since this is a relatively coarse resolution, trajectories passing through areas of high wind shear will have a higher level of uncertainty.

We apply these techniques to study a recently developed meteorological theory [4] proposing that hurricanes develop in protected "marsupial" pouches. We examine trajectories seeded near developing hurricanes for evidence that they are protecting the storm's core from outside influence.

2 RELATED WORK

While the methods and error analysis of numerical integration are well established for analytic differential equations, work on other sources of error in discrete schemes is relatively recent. Lopes and Brodlie [3] formulated a framework for describing sources of error in flow visualization, including interpolation inaccuracy in discrete fields, but did not perform any numerical analysis. Darmofal and Haimes [11] analyzed error arising from temporal interpolation of time-varying vector fields that are sampled discretely in time, but did not address the effects of spatial interpolation. Finally, Shirayama [12] empirically investigated integration errors introduced by temporal and spatial interpolation in fully sampled vector fields. In this paper we present a simple upper bound on particle tracing inaccuracy due to the lack of information between sampling points in a discrete time-varying vector field.

The visualization community has developed generic techniques for incorporating local and accumulated uncertainty in visualizations of flow trajectories, such as those by Wittenbrink et al [9] and Pang et al [10]. In the end, we map total trajectory uncertainty inversely to line thickness.

Application-wise, the above work has not previously been implemented into a unified product available to meteorologists. NOAA's HYbrid Single-Particle Lagrangian Integrated Trajectory (HYSPLIT) model [5] handles a wide variety of scenarios, but is a closed source package that is cumbersome to build upon, is not interactive, and is difficult to use with arbitrary data sources. The Grid Analysis and Display System (GrADS) [6] allows input from a variety of data sources, but its trajectory routines are in only two dimensions. Other meteorologists use custom-built trajectory generation software in languages such as IDL, but they are not publicly available. In the end, we decided to build upon Unidata's Java-based Integrated Data Viewer. It is an open-source package that handles a variety of data formats and coordinate systems, along with providing existing visualization routines that allow our trajectories to be shown in a multi-field context.

3 METHODS

Trajectory generation methods typically use the fourth-order Runge-Kutta integration scheme, and we are no different. These trajectories

can be run forward or backward in time, determining the future or past locations, respectively, of the user-specified seeds.

Regardless of the numerical integration technique chosen, there is an inherent uncertainty in the underlying data. The discrete vector field represents a sampling of a continuous velocity distribution, and between sample points we do not know the value of the distribution. In a regular spatio-temporal sampling grid, the unit cell is a four-dimensional hypercube, with one sample point at each of its 16 corners (see figure 1). While *a priori* knowledge of fluid flow may indicate that linear interpolation is a better estimate of the velocity within the hypercube than the nearest neighbor, and that quadratic or cubic interpolation are better than linear, the true distribution is unknown. We wish to estimate bounds on the possible values of the distribution within one hypercube based on the values at the corners.
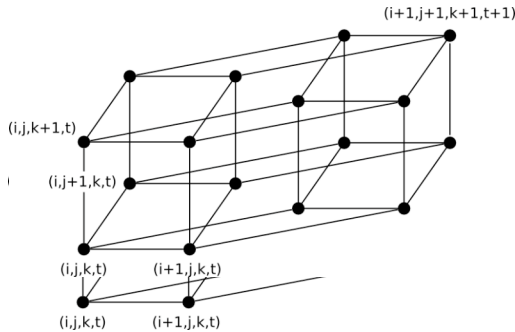
Figure 1: A cell of the spatio-temporal sampling grid. Sampled velocities are known at each of the corners of the hypercube (black dots), but the value of the distribution within the hypercube is unknown. Certain illustrative sample points are labeled with their sampling indices.

Our estimate consists of the assumption that, at any point in the interior of the hypercube, each component of the true velocity is bounded by its extreme values among all the surrounding corner points:

$$\hat{v}_i(x) \equiv \{\tilde{v}_i(y) \mid y \in N(x)\}$$
$$v_i(x) \in [\min(\hat{v}_i(x)), \max(\hat{v}_i(x))]$$

Here, *N(x)* is the set of corner points of the hypercube containing the point *x*.

In each component of the velocity, the trajectory that deviates the most from the trajectory computed from interpolated values results from integrating a constant vector field that takes on one of the extreme values identified by the bound. Therefore, with two choices per component and three components to the velocity vectors, we may test eight different combinations of extreme values to find the trajectory within each hypercube that differs most from the trajectory computed from interpolated values, which we call the "main" trajectory. This difference is taken to be an upper bound on our uncertainty in the main trajectory.

Computing the aggregate uncertainty over the course of the entire length of a trajectory requires $O(8^n)$ computations for a trajectory that passes through *n* hypercubes, since we must consider all extreme directions that the worst-case trajectory could take at every hypercube boundary. Instead we estimate this value in $O(n)$ by considering diverging trajectories of a fixed time length *s*; for a main trajectory of time length *S*, we compute *S/s* diverging trajectories. We estimate the aggregate uncertainty by *S/s* times the maximum distance any diverging trajectory achieves from the main trajectory.

We represent this computed uncertainty through the trajectory's thickness: thinner lines are less certain than their thick counterparts. We chose this mapping to allow the more certain lines to visually dominate the scene, while demoting the less certain ones to a less-prominent role. This decision is arbitrary, though, as it can be argued that the reverse mapping is more intuitive since thicker lines could represent a larger possible range of positions for the given pathline.

To better understand the physical makeup of the air parcels over time, the trajectories can be marked according to user-specified properties. For the purpose of this study, we color each pathline segment based upon the humidity at the point in time it passed through its local space. This enables a series of "snapshots" over time to be displayed in a single frame. Since these visualization structures paint an aggregate picture of the physical processes over time, more temporal detail can be provided, as necessary. In a manner similar to Sobel et al's particle flurries [8], we paint only a portion of the trajectories at a given time step. In their case, the main goal is to reduce occlusion, while ours is to provide an indication of the leading edge of each trajectory at that given point in time. This concept is shown in Figure 2.

To aid in the analysis, other meteorological variables (i.e., temperature, pressure) can be viewed simultaneously using a palette of traditional visualization techniques (plan and cross-sectional contour/color plots, isosurface and volume rendering, vector and streamline plots, etc). These plots are synchronized in time with the trajectories' current position, as shown in Figure 2. In effect, this provides a reference frame to the location of the hurricane, aiding in understanding the relationship between air parcel and storm movement.
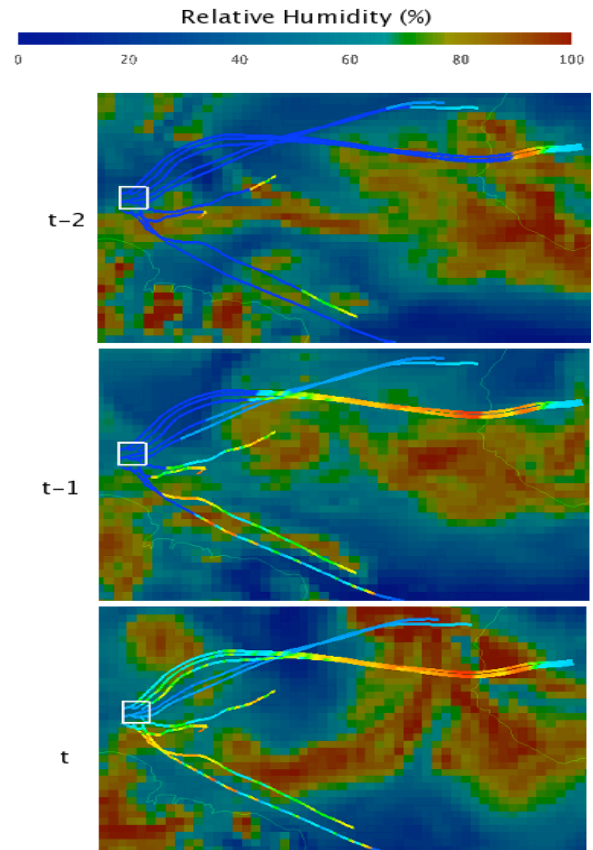
Figure 2: Underlying, synchronized 2-D color plot shows relative humidity field over time, aiding in understanding the pathlines' context. Pathlines seeded by user in white ROI travel back through time; pathline segments are colored according to snapshots of relative humidity; dark blue segments have not yet been "reached" in the currently shown time range.

These methods were all geared toward addressing meteorological questions related to better understanding the development of hurricanes. Specifically, we wanted to test the validity of a recently devised theory proposing that hurricanes develop in a "pouch" of relatively isolated air that travels with the storm. Another test was to search for sources of dry air that may inhibit hurricane development. The Saharan Desert is one well-studied source of dry air [7], but another source of dry air can come from mid-latitude air to the north. Since wind shear may be present in both of these cases, we use uncertainty representations to gain a deeper understanding of the underlying data and quickly prune unlikely results.

4 RESULTS

In the 2-D example shown in Figure 3, the effects of horizontal wind shear are shown on the trajectories that pass through it. It is immediately clear that the pathlines near the center of the image are less likely to be reliable.
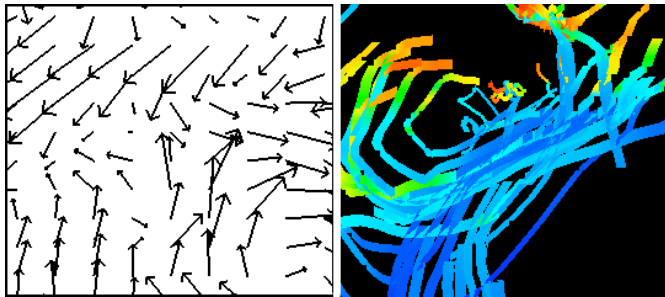
Figure 3: Using uncertainty to show effects of wind shear on trajectories, facilitating quick visual pruning of unlikely results. One time step from the wind field (left) used to generate the pathlines at right. Color represents relative humidity "snapshots" as in Figure 2. Note wind shear at center of field (neighboring vectors in nearly opposite directions) and its effect on trajectory confidence (thinner lines are less certain). This also eliminates the need to examine the underlying vector field for wind shear at all time steps since each pathlines' uncertainty encompasses the entire range.

To address the meteorological question of whether external air systems can affect the developing core of a hurricane, we generated trajectories from data near hurricanes Isabel (2003), Ivan (2004), and Helene (2006). Our work is still too preliminary to draw scientific conclusions, but it does show some evidence to support the marsupial paradigm.

In Figure 4, air parcels released near Hurricane Isabel show two distinct groups of trajectories. Trajectories released from dry areas originate from the Sahara and descend from higher, drier levels. Trajectories released from within the core of the storm originate from lower levels and spiral into the core of the storm from below. The results support the idea of the storm core being protected from the drier surrounding air since no trajectories started within the moist core region come from the drier mid- to upper-level Saharan region. Similar results were obtained for Ivan and to an extent, for Helene. However, in Helene, as shown in Figure 5, a dry air intrusion is seen to extend into the storm from the south and west. The air to the west is found to originate from the east, and likely the Sahara, but comes from a higher level and descends as the air reaches the western side of the storm. Whether this dry air gets into the inner core of the storm cannot be determined from the coarse-resolution analyses.
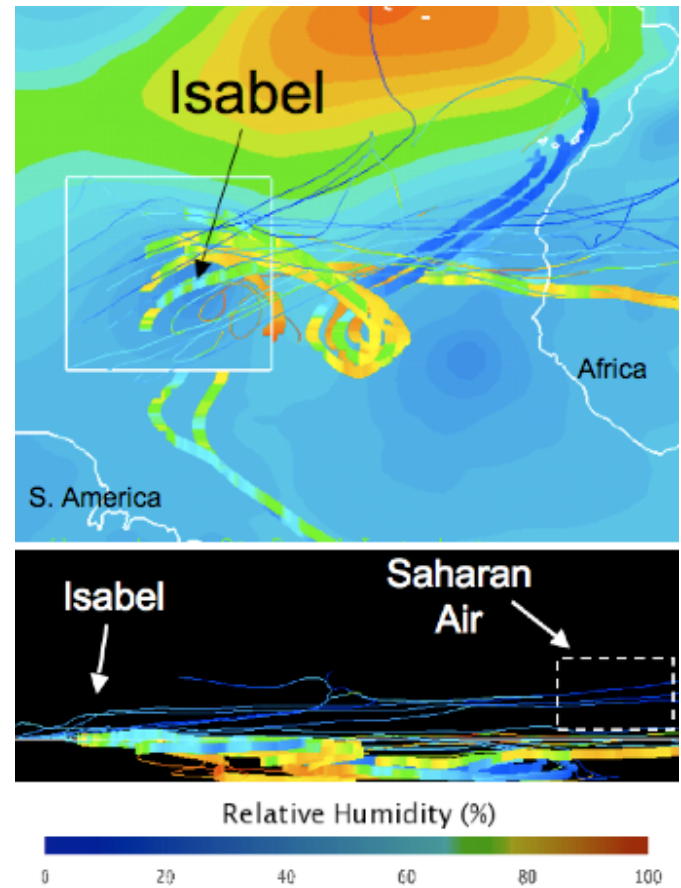
Figure 4: Overhead and side views of trajectories producing evidence supporting the proposed marsupial paradigm. Air parcels in white box are released around Hurricane Isabel at a height of 700mb. Dry air (blue trajectories) originates above this level and does not enter the interior of the hurricane, while moist air (warmer-colored trajectories) originates at lower levels, moves into the storm circulation, and sprials up into the moist region in Isabel. Line thickness indicates path of dry air is generally more uncertain than that of warm air. Background contour plot shows geopotential height (height of pressure surface).

When the uncertainty of these trajectories is computed, it paints an unexpected picture. The low-level trajectories pass through the high-gradient regions of the storm while the mid-level trajectories of Saharan origin are moving through the environment where we usually presume the fields to vary far less. As a result, the low-level trajectories should have encountered greater horizontal shear of the wind, but perhaps that is not the case and is something to investigate further.
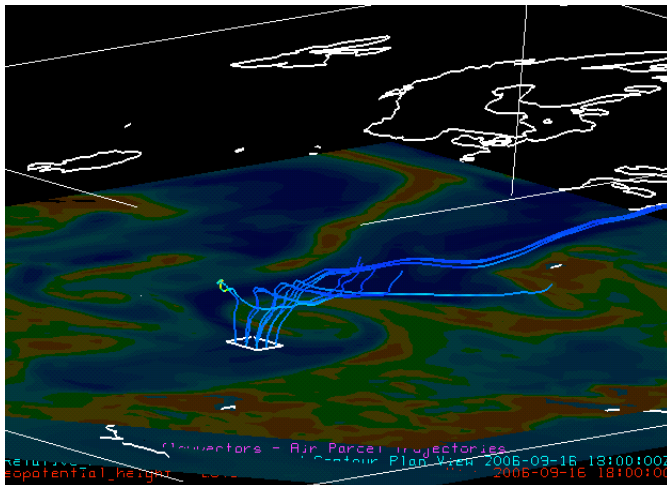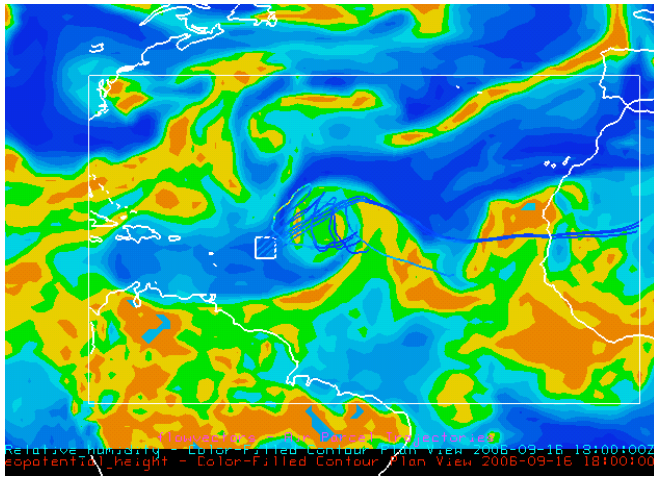
Figure 5: Overhead and perspective views of dry air, mostly from the Saharan Desert, entering Hurricane Helene's storm system (center of top image) from above. This type of intrusion does not support the marsupial paradigm. Background contour plot shows relative humidity levels.

We then addressed the other meteorological question of looking for sources of dry air not of Saharan origin that might affect hurricane development. In examining data from Helene and Isabel, the search proved to be fruitless, as no sources of dry air from mid-latitudes were found. While this is a preliminary search, it is noteworthy since it reinforces the traditional belief that the Saharan Desert is often the source of dry air.

5   CONCLUSIONS

The original goal of this work was to improve the understanding of the local environment of developing hurricanes. To that end, we have enabled the efficient generation and analysis of three-dimensional meteorological trajectories. We have derived an upper bound on the uncertainty associated with these trajectories due to interpolation error. We have also shown preliminary evidence to support a new meteorological theory that proposes hurricanes develop within protected pouches of atmosphere.

Our short-term goal for this work is to continue using the tool to draw more conclusive evidence to support or refute the marsupial paradigm. We also would like to more formally evaluate the utility of uncertainty visualization in this process.

In the longer term, we plan to use the tool with higher-resolution data and use uncertainty in a different manner: instead of having interpolation uncertainty from coarse grid spacing, it may display interesting results with small-scale features. We will initially

test regions near updrafts and use the uncertainty to understand the potential for air parcels to enter them.

Finally, we will explore the option of obtaining intermediate values that are generated when the model data is being computed. These values could be very useful for our own uncertainty calculations since we currently need to make assumptions about the model's inner workings.

REFERENCES

[1]   Chen, L.W.A., Doddridge, B.G., Dickerson, R.R., Chow, J.C., Henry, R.C., 2002. Origins of fine aerosol mass in the Baltimore-Washington corridor: implications from observation, factor analysis, and ensemble air back trajectories. *Atmospheric Environment* 36, 4541–4554.

[2]   Johnson, C. R. and Sanderson, A. R. 2003. A Next Step: Visualizing Errors and Uncertainty. *IEEE Comput. Graph. Appl.* 23, 5 (Sep. 2003), 6-10.

[3]   A. Lopes and K. Brodlie, "Accuracy in 3D Particle Tracing," Mathematical Visualization: Algorithms, Applications and Numerics, HC Hege and K. Polthier, eds., *Springer Verlag*, 1998, pp. 329-341.

[4]   Dunkerton, T. J., M. T. Montgomery, and Z. Wang, 2008: Tropical Cyclogenesis in a Tropical Wave Critical Layer: Easterly Waves. Atmospheric Chemistry and Physics (submitted).

[5]   Draxler, R.R., Rolph, G.D., 2003. HYSPLIT (Hybrid Single-Particle Lagrangian Integrated Trajectory) Model access via NOAA ARL READY Website (http://www.arl.noaa.gov/ready/hysplit4.html).NOAA Air Resources Laboratory, Silver Spring, MD.

[6]   Berman, F., Chien, A., Cooper, K., Dongarra, J., Foster, I., Gannon, D., Johnsson, L., Kennedy, K., Kesselman, C., Mellor-Crumme, J., Reed, D., Torczon, L., and Wolski, R. 2001. The GrADS Project: Software Support for High-Level Grid Application Development. Int. J. High Perform. Comput. Appl. 15, 4 (Nov. 2001), 327-344.

[7]   Karyampudi, V.M., and T.N. Carlson, 1988: Analysis and Numerical Simulations of the Saharan Air Layer and Its Effect on Easterly Wave Disturbances. J. Atmos. Sci., 45, 3102–3136.

[8]   Sobel, J. S., Forsberg, A. S., Laidlaw, D. H., Zeleznik, R. C., Keefe, D. F., Pivkin, I., Karniadakis, G. E., Richardson, P., and Swartz, S. 2004. Particle Flurries: Synoptic 3D Pulsatile Flow Visualization. IEEE Comput. Graph. Appl. 24, 2 (Mar. 2004), 76-85.

[9]   C.M. Wittenbrink, A. Pang, and S.K. Lodha, "Glyphs for Visualizing Uncertainty in Vector Fields," IEEE Trans. Visualization and Computer Graphics, vol. 2, no. 3, Sept. 1996, pp. 266-279.

[10]   A.T. Pang, C.M. Wittenbrink, and S.K. Lodha, "Approaches to Uncertainty Visualization," The Visual Computer, vol. 13, no. 8, Nov., 1997, pp. 370-390.

[11]   Darmofal, D. L. and Haimes, R. 1996. An analysis of 3D particle path integration algorithms. J. Comput. Phys. 123, 1 (Jan. 1996), 182-195.

[12]   Shirayama S. Processing of computed vector fields for visualization. J Comput Phys 1993;106:30–41.